Progress in Neuropsychopharmacology & Biological Psychiatry 101 (2020) 109939

Contents lists available at ScienceDirect

Progress in Neuropsychopharmacology & Biological Psychiatry

journal homepage: www.elsevier.com/locate/pnp

Optimized integration of fluoxetine and 7, 8-dihydroxyflavone as an efficient therapy for reversing depressive-like behavior in mice during the perimenopausal period

Nashwa Amin[a,b,1], Shiyi Xie[c,1], Xiaoning Tan[a,1], Yili Chen[d,1], Qiannan Ren[a], Benson O.A. Botchway[a], Shaohua Hu[e], Yongchun Ma[f], Zhiying Hu[g,**], Marong Fang[a,*]

[a] Institute of Neuroscience and Gastrointestinal Laboratory, The children's Hospital, Zhejiang University School of Medicine, Hangzhou, China
[b] Department of Zoology, Faculty of Science, Aswan University, Egypt
[c] The Second Clinical Medical College of Zhejiang Chinese Medical University, Hangzhou, China
[d] Department of Neurosurgery, The Fourth Affiliated Hospital, Zhejiang University School of Medicine, Yiwu, China
[e] Department of Psychiatry, First Affiliated Hospital, Zhejiang University School of Medicine, Hangzhou, China
[f] Tongde Hospital of Zhejiang province, China
[g] Obstetrics & Gynecology Department, Zhejiang Integrated Traditional and Western Medicine Hospital, Hangzhou, China

ARTICLE INFO

Keywords:
Autophagy
Brain-derived neurotrophic factor (BDNF)
Inflammation
Perimenopausal depression
Tropomyosin-related kinase B

ABSTRACT

Fluoxetine (FLX) has been considered as an effective anti-depressant drug. Besides, previous studies reported reasonable anti-depressant effects for 7, 8-dihydroxyflavone (7, 8 DHF). However, the combination of FLX and 7, 8 DHF in a well-established depression model has not been explored. In this study, we demonstrate that the 7, 8 DHF can improve the anti-depressant efficacy of FLX in a chronic unpredictable mild stress (CUMS)-induced depression during the perimenopausal period. The corresponding mechanism of FLX + 7, 8 DHF therapy and the effect of ANA-12 are also investigated. Moreover, the influences of 7, 8 DHF (5 mg/kg/day), FLX (18 mg/kg/day), and ANA-12 (0.5 mg/kg/day) on a depressive-like behavior are displayed. Inflammatory, autophagic and apoptotic changes of hippocampus and cortex are examined by using western blot, immunofluorescence, and Real-Time Quantitative reverse transcription-polymerase chain reaction (RT-qPCR) techniques. The protein levels of phosphatidylinositol 3 kinase (PI3K)/ protein kinase B (Akt)/mechanistic target of rapamycin (mTOR)/ phosphorylated extracellular signal-regulated kinase1/2 (p-ErK 1/2)/brain-derived neurotrophic factor (BDNF)/ tropomyosin-related kinase B (TrkB) of hippocampus and cortex are assessed by western blot. The combined FLX and 7, 8 DHF treatment can significantly improve depressive-like behavior in sucrose preference and forced swimming tests accompanied by a noticeable upregulation of autophagy, neuronal nuclei (NeuN), ionized calcium-binding adaptor molecule 1 (Iba1) expressions, and PI3K/Akt/ mTOR/ p-ErK 1/2 signaling pathways. Besides, an obvious increase of the brain-derived neurotrophic factor (BDNF) and TrkB levels are observed with down-regulated inflammation and apoptosis. These findings suggest that the integrated FLX and 7, 8 DHF holds a potential as an efficient treatment to ameliorate depressive-like behavior in perimenopausal patients.

1. Introduction

Currently, depression is one of the most crucial psychiatric disorders. Life-style, biological changes, and various events existed during daily life can induce depression behavior [Fiske et al., 2009; Greenberg et al., 1993]. Depression can be characterized by cellular and molecular alterations generated through a circuit of neural substrates [Krishnan and Nestler, 2008]. Moreover, depressive behavior considerably varies according to gender and changes in sexual hormones. Alongside, the possibility of developing perimenopausal depression in women can be largely increased by the volatility in levels of the estrogen hormone [Borrow and Cameron, 2014]. Perimenopause refers to the transient time between reproductive and non-reproductive life, and the function of ovarian follicles during such period is diminished [Greendale et al.,

* Correspondence to: M. Fang, Institute of Neuroscience and Gastrointestinal Laboratory, The children's Hospital, Zhejiang University School of Medicine, 866 Yuhangtang Road, Hangzhou 310058, China.
** Correspondence to: Z. Hu, Department of Obstetrics & Gynecology, Zhejiang Integrated Traditional and Western Medicine Hospital, Hangzhou 310003, China.
E-mail addresses: huzhiying@zcmu.edu.cn (Z. Hu), fangmaro@zju.edu.cn (M. Fang).
[1] These authors contributed equally.

https://doi.org/10.1016/j.pnpbp.2020.109939
Received 10 December 2019; Received in revised form 19 March 2020; Accepted 29 March 2020
Available online 01 April 2020

2011]. This malfunction can reduce the estrogen and progesterone hormone levels and increase follicle stimulating hormone (FSH) levels. Vasomotor instability [Davis et al., 2015], irregularity in menstrual cycle [Prior, 2005], cognitive [Amin et al., 2006], metabolic (Janssen et al., 2008], and somatic changes [Perez-lopez et al., 2014] are the common side effects of the above mentioned malfunction. During the perimenopausal period, a variety of symptoms such as cognitive dysfunction, anxiety, and irritability are manifested [Greendale et al., 2011]. Brain-derived neurotrophic factor (BDNF) and tropomyosin receptor kinase B (TrkB) expressions are greatly impacted by the hormonal status. Previous studies demonstrated the BDNF expression in the olfactory bulb [Jezierski and Sohrabji, 2001], hippocampus [Singh et al., 1995], cortex [Sohrabji et al., 1995], amygdala [Zhou et al., 2005] to be augmented via the replacement of estrogen in young adult ovariectomized female rats. The occurrence of depressive symptoms on a patient minimizes the BDNF content, synthesis, and release [Harte-Hargrove et al., 2013]. Thus, depressed mice have a lower level of BDNF expression. As a receptor for BDNF, TrkB showed a critical role in modulating an effective signaling pathway for neural plasticity, survival, and growth. BDNF-induced TrkB activation is widely expressed in adult mammalian brain and essential for synaptic plasticity [Choo et al., 2017]. Selective serotonin reuptake inhibitors (SSRIs) have been emerged as promising antidepressant drugs for effective treatment of depression [Marken and Munro, 2000]. The pathway of these antidepressant drugs relies on the increase of serotonin levels in the synaptic cleft via preventing serotonin reabsorption by presynaptic neuron [Hiemke and Hartter, 2000]. Among all, fluoxetine (FLX) has received an increasing interest as one of the most efficient antidepressant drugs [Tan et al., 2018]. Our previous studies elucidated the antidepressant effects of FLX via the regulation of apoptosis, autophagy, and upregulation of brain-derived neurotrophic factor (BDNF) expression [Yang et al., 2017; Tan et al., 2018]. In perimenopausal depression, SSRIs (such as FLX) have been commonly used as a first choice. Serotonin noradrenaline reuptake inhibitors (SNRIs) come into play following the inefficaciousness of the SSRI. As with most clinically used drugs, both SNRIs and SSRIs can exacerbate the anxiety and irritability features that have been associated with perimenopausal depression [Dunlop and Davis, 2008]. 7, 8-dihydroxyflavone (7, 8 DHF) can be found in plants and its antidepressant effect has been evidenced experimentally in animal models of depressions [Tatiana et al., 2019; Zhang et al., 2016]. For example, Zhang and colleagues found that the anti-depressant effect of 7, 8DHF can be mediated via upregulation of synaptic protein expressions [Zhang et al., 2016]. Furthermore, several studies investigated the anti-depressant effects of FLX and 7, 8 DHF individually, however, the effect of the combination of these two drugs has not been reported yet.

Herein, the therapeutic impact of the combined FLX + 7, 8 DHF to ameliorate depressive-like behavior during perimenopausal period was investigated. We performed bilateral ovariectomy on mice, instigated the depressive-like behavior using the chronic unpredictable stress model (CUMS), and administered drugs for 28 days. Then, the behavioral and biochemical changes were examined. The anti-depressant mechanism of the optimized treatment was also described. Results evidenced that the integrated FLX + 7, 8 DHF drug has a good capability to alleviate perimenopausal depression through up-regulation of PI3K/AKT/mTOR and Erk1/2, and sequentially stimulation of BDNF/TrkB signal.

2. Materials and methods

2.1. Animals

Thirty- five adult female C57BL/6J mice (average weight of 20 ± 1 g) obtained from the animal center of Zhejiang University Medical College were used in this study. The mice were allowed to eat and drink freely at a room temperature (24 ± 1 °C) under a relative humidity of 55% for 12 h light/12 h dark cycle. All experiments and animal treatments were optimized according to the guidelines for the care and use of laboratory animals established by the National Institutes of Health, and approved by the Ethics Committee of Zhejiang University Medical College.

2.2. Animal groups and drug administration

Mice were randomly divided into seven (7) groups: Control, DMSO, FLX, 7, 8 DHF, FLX + 7, 8 DHF, ANA-12 and FLX + ANA-12. Modified bilateral ovariectomy was performed in all mice, which was followed by chronic unpredictable mild stress (CUMS). The control group were exempted from the CUMS. 1% DMSO (thermofisher, 85,190) was injected intraperitoneally at dose 5 mg/kg/day. Fluoxetine (Patheon France, lot J20050122) was dissolved in 0.9% physiological saline to a concentration of 2 mg/mL. FLX was intragastrically administered at dose 18 mg/kg/day in the respective groups (FLX, FLX + 7, 8 DHF and FLX + ANA-12) (Krishna et al., 2017; Cazorla et al., 2011). 7, 8 DHF (Selleck, Lot. S831901) was dissolved in 1% DMSO to a concentration of 1 mg/mL, and delivered intraperitoneally (5 mg/kg/day) (Agacayak et al., 2015). In the FLX + 7, 8 DHF mice, 7, 8-DHF was administrated three hours after FLX injection (Willner et al., 1987). ANA-12 (Selleck, lot No. S774501) was dissolved in 1% DMSO to a concentration of 0.1 mg/mL, and intraperitoneally administered at dose 0.5 mg/kg/day (Willner et al., 1987). In the FLX + ANA-12 mice, ANA-12 was administrated 3 h following FLX injection (Willner et al., 1987). All drugs were administrated one hour prior to the stress experiment for 28 days.

2.3. Perimenopausal model

Bilateral ovariectomy was performed as previously described (Zhu et al., 2019). Briefly, ether anesthesia was given to mice via inhalation (1 mL/min). A midline abdominal incision was performed at the pelvic level. The first side of the ovary was surgically removed and a week later, the other side was surgically removed. The experimental timeline is illustrated in (Scheme 1).

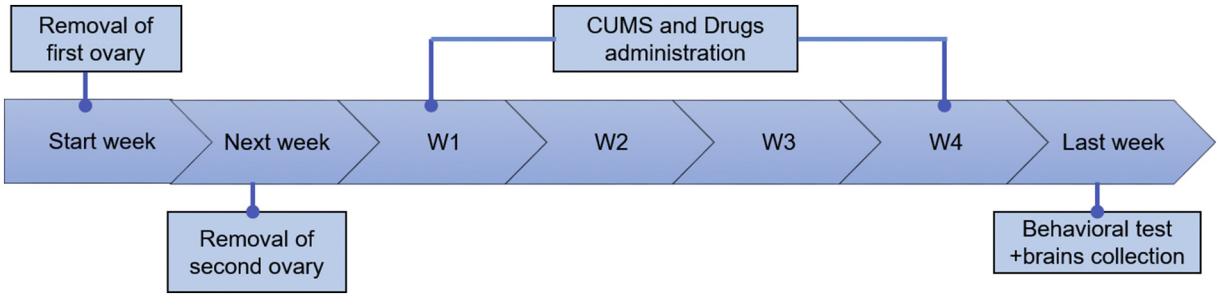

Scheme 1. Representative diagram for the experiment time schedule.

Table 1
Chronic unpredictable mild stress schedule.

Day 1	Day 2	Day 3	Day 4	Day 5	Day 6	Day 7
Suspension 90 min	Forced swimming 5 min in water at 25 °C	Behavioral restraint 4 h	Restricted access to food 24 h	Tail clamping 3 min	Continuous lighting overnight	Restricted access to water 24 h
Day 8	Day 9	Day 10	Day 11	Day 12	Day 13	Day 14
Behavioral restraint 5 h	White noise (80 dB) 3 h	Restricted access to water 24 h	Cage tilt (45°) 24 h	Forced swimming 5 min in water at 25 °C	Restricted access to food 24 h	Wet padding 24 h
Day 15	Day 16	Day 17	Day 18	Day 19	Day 20	Day 21
Continuous lighting overnight	Restraint shock 30 min	Tail clamping 6 min	Behavioral restraint 6 h	Wet padding 24 h	Restraint shock 30 min	Forced swimming 5 min in water at 4 °C
Day 22	Day 23	Day 24	Day 25	Day 26	Day 27	Day 28
Restricted access to water 24 h	Cage tilt (45°) 24 h	Forced mint scent 3 h	Strong light 30 min	Forced swimming 5 min in water at 45 °C	Continuous lighting overnight	Restricted access to food 24 h

2.4. Chronic unpredictable mild stress (CUMS)

One week after the removal of ovaries, coupled with routine feeding, mice were randomly exposed to several stressors [Zhu et al., 2019; Can et al., 2012]. The stressors employed in this study are shown in Table 1. The CUMS experiment was done for 28 days.

2.5. Behavioral test

2.5.1. Forced swimming test (FST)

Mice were individually placed in a cylinder of water (temperature: 24 ± 1 °C), and allowed to swim for 6 min under normal light exposure. The water depth was carefully adjusted to prevent mice from touching the bottom of the cylinder with either tail or hind limbs. The behavior of mice was video recorded, and the immobility time in the last 4 min test period was recorded. The immobility time represented the duration when the mouse either remained floating or was motionless, with a very slight movement in order to ensure its balance in water [Liu et al., 2018].

2.5.2. Sucrose preference test (SPT)

Mice were accustomed to two bottles of water, which was followed by two bottles of 2% sucrose for a day. Then, water deprived for 23 h, and mice were exposed to one bottle of 2% sucrose, and one bottle of water for 2 h (bottle positions switched after 1 h). The total consumption of both water and sucrose were measured, and the sucrose preference was optimized as the average sucrose consumption ratio during 2 h. The sucrose consumption (%) was defined as the percentage of sucrose consumption to the total consumption of both water and sucrose within 2 h[Koo et al., 2010].

2.6. Immunofluorescence

Mice were anesthetized with 10% chloral hydrate, transcardially perfused with 50 mL (±) of 0.9% saline to flush the vascular blood, and then perfused with 4% paraformaldehyde in 0.01 M phosphate-buffered saline (PBS, pH 7.4). Brain tissues were obtained after perfusion, and fixed with 4% paraformaldehyde. On the next day, tissues were transferred into a 30% sucrose solution. Embedding in OCT and frozen tissue section were performed using a freezing microtome (Leica, Wetzlar, Germany). Frozen sections of 18 um thickness were dried at 37 °C, and then blocked with 5% normal goat serum at room temperature for 1 h. After, primary antibodies were added in the following concentrations at 4 °C overnight: NeuN (Abcam, 1:1000), Iba1 (Abcam, 1:100), LC-3II (CST, 1:200) and GFAP (CST, 1:200). Regarding the negative control sections, 0.01 M PBS was used to replace the primary antibody. On the following day, the sections were washed with 0.01 M PBST for 5 min three times, and then incubated with secondary antibody containing FITC goat anti-rabbit IgG (1:100, Boster, BA1105), Alexa Fluor anti-mouse 594 and Alexa Fluor® anti-rabbit 488 for 3 h at room temperature. The section were then washed with 0.01 M PBS three times. A mounting medium containing DAPI (VECTASHIELD, USA) was added to the slides, and covered with coverslips for observation. Slides were observed under a fluorescence microscope (Olympus BX51, NIKON, Japan) at excitation/emission wavelengths of 547/570 nm (Cy3, red), 494/520 nm (FITC, Green), and 360/460 nm (DAPI, blue). Images were taken at 200× magnification.

2.7. Western blotting

The total proteins of hippocampus and cortex brain tissues were extracted with 1% PMSF (Phenylmethanesulfonyl fluoride, Beyotime ST505) in 1 mL of ice-cold RIPA buffer, with added protease inhibitor cocktail EDTA-free and phosphatase inhibitors. After homogenizing, and centrifuging at 12000 rpm for 20 min at 4 °C, supernatant proteins were preserved at −80 °C. Sample concentrations were determined

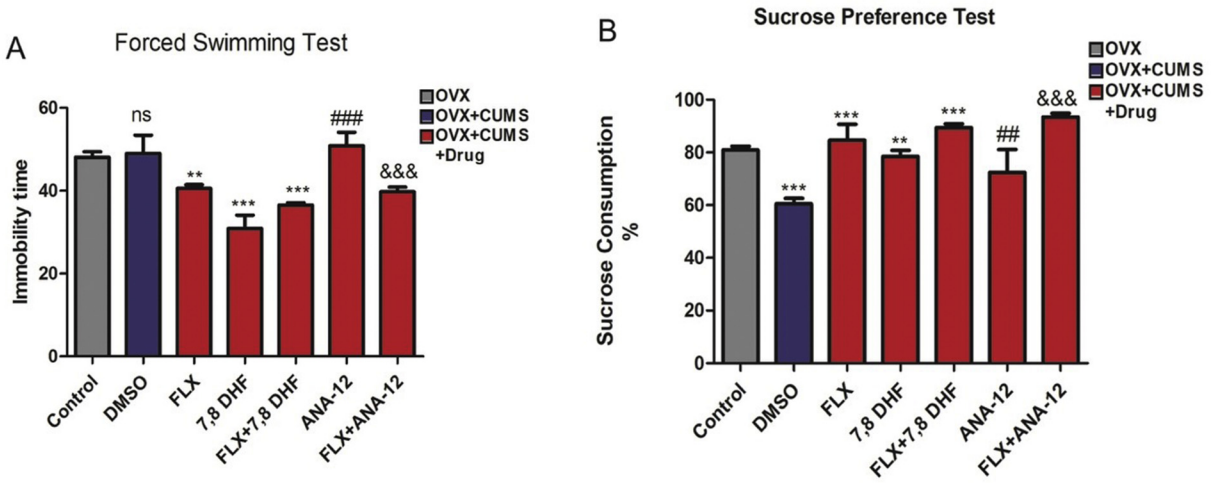

Fig. 1. An integrated treatment of FLX+7, 8 DHF reverses the depressive symptoms in mice during the perimenopausal period. All values are expressed as mean ± SEM. (A) Forced swimming test; ($F_{6, 13}$ = 17.686), DMSO vs. control: P = ns, FLX vs. DMSO& control: $^{**}P < .01$, 7,8 DHF & FLX+7, 8 DHF vs. DMSO& control: $^{***}P < .001$, ANA-12 vs. FLX+7, 8 DHF: $^{\#\#\#}P < .001$, FLX + ANA-12 vs. ANA-12: $^{\&\&\&}P < .001$. (B) Sucrose preference test; ($F_{6, 14}$ = 6.639), DMSO vs. control: $^{***}P < .001$, FLX, 7, 8-DHF & FLX+7, 8 DHF vs. DMSO: $^{***}P < .001$, ANA-12 vs. FLX+7, 8 DHF: $^{\#\#}P < .01$, FLX + ANA-12 vs. ANA-12:$^{\&\&\&}P < .001$.

with BCA kits (KeyGEN, Nanjing, China). The protein (20 μg) from each sample was subjected to electrophoresis on 15% SDS PAGE gel using a constant voltage (200 V) for 60 min. The proteins were transferred to a polyvinylidene difluoride (PVDF) membrane with the Bio-Rad Trans Blot apparatus. Thereafter, membranes were blocked with TBST containing 5% non-fat milk for 2 h at room temperature. Membranes were incubated with primary antibody overnight at 4 ˚C. The primary antibodies used were: rabbit polyclonal antibody against GAPDH (CST, 1:1000), ATG5/ATG12 (Abcam, 1:1000), BDNF (Abcam, 1:1000),TrkB (Abcam,1:1000), Beclin-1 (CST, 1:1000), LC-3II (CST, 1:1000), mTOR (Abcam, 1:1000), AKT (CST, 1:1000), P44/42-MAPK (ERK1/2) antibody (CST,1:1000), PI3K (Boster,1:500), inducible nitric oxide synthase (iNOS) (Boster, 1:100), and nuclear factor kappa B (NF-κB) (CST, 1:1000), Bcl-2 (Abcam,1:1000),Bax(Abcam,1:1000). On the following day, the membrane was washed with TBS containing 0.05% Tween 20 (TBST). After washing 3 times, with each wash lasting 5 min, membranes were incubated with goat anti-rabbit and anti-mouse IgG antibody (BOSTER, 1:5000) at room temperature for 2 h, and then washed with TBST 3 times (each wash lasting 5 min). Membranes were then exposed to hyper-film detection after incubating with the ECL system. The grayscale value of each band was analyzed using the Image Lab software. Each experiment was performed three times.

2.8. Real-time PCR

Real-time PCR was conducted to detect RNA expression level of ATG5 and LC3 in the hippocampus. The Trizol (Invitrogen) extraction reagent was used to extract hippocampal RNA. All procedures were carried out according to the manufacturer's instruction. The concentration and purity of RNA samples were determined by Thermo NanoDrop 2000. One microgram of RNA from each sample was reverse transcripted into cDNA, according to the instructions of the DBI-2220 Bestar qPCR RT Kit. Real-time PCR specific primers for mouse ATG5 and β-actin (internal control) were designed using Primer Express software.

The primers used were as follows:

β-actin Forward: 5′- CTGTCCCTGTATGCCTCTG -3′.

β-actin Reverse: 5′- ATGTCACGCACGATTTCC -3′.

ATG5 Forward: 5′- AACTGAAAGAGAAGCAGAACCA -3′.

ATG5 Reverse: 5′-TGTCTCATAACCTTCTGAAAGTGC -3′.

LC3 Forward: 5′-GAGAAGCAGCTTCCTGTTCTGG-3′.

LC3 Reverse: 5′-GTGTCCGTTCACCAACAGGAAG-3′;

Real-time PCR protocol was done following instructions from DBI-2044 Bestar SybrGreen qPCR master mix. The reaction program for the PCR was as follows: 50 ˚C for 2 min; 95 ˚C for 10 min; 40 cycles of 95 ˚C for 5 s, 55 ˚C for 30 s, and 72 ˚C for 30 s. All mRNA expression levels were detected by RT-PCR. Results were analyzed using Biorad CFX manager program, version 3.0. Each experiment was done three times.

2.9. Statistical analysis

Data were analyzed by one-way ANOVA using SPSS 20.0, followed by post hoc Fisher's least significant difference (LSD) tests. The *P* values less than 0.05 were considered statistically significant. Histograms were generated in GraphPad Prism 5. Behavioral test, western blotting, and immunofluorescence data are expressed as mean ± SEM. Gray values of western blot results were calculated using Image Lab. Immunofluorescence results of Neun Iba1, LC3 and GFAP were analyzed by Pro Image Plus. $^{*}P < .05$, $^{**}P < .01$, $^{***}P < .001$ was determined as statistically significant, where * symbol was the difference between the DMSO, control, FLX, 7, 8 DHF and FLX+7, 8 DHF groups, # symbol was the difference between the ANA-12 and FLX+7, 8 DHF groups and the difference between the FLX + ANA-12 and ANA-12 groups is denoted by & symbol.

3. Results

3.1. An integrated treatment of FLX+7, 8 DHF reverses the depressive symptoms in mice during the perimenopausal period

Medical conditions can alter the behavioral function of affected individuals. Hence, the improvement in behavioral test after drug administration proves the effectiveness of medicinal agent. Herein, SPT and FST were conducted to observe the behavioral changes of mice after 28 days of drug administration. The FST displayed a shorter immobility time ($F_{6, 13}$ = 17.686) in 7, 8 DHF and FLX+7, 8 DHF groups than that of the DMSO and control groups ($P < .001$). Moreover, the FLX group exhibited a significant decrease in immobility time compared to both control and DMSO groups ($P < .01$). The ANA-12 group revealed an increment of the immobility time in comparison to the FLX +7, 8 DHF group ($P < .001$), while the FLX + ANA-12 group showed a reduced immobility time ($P < .001$) (Fig. 1A).

The sucrose consumption was obtained by SPT as illustrated in Fig. 1B. It can be seen that the sucrose consumption of FLX, FLX+7, 8 DHF and FLX + ANA-12 groups was higher that of DMSO group ($P < .001$) ($F_{6, 14}$ = 6.639). Meanwhile, the ANA-12 group showed a

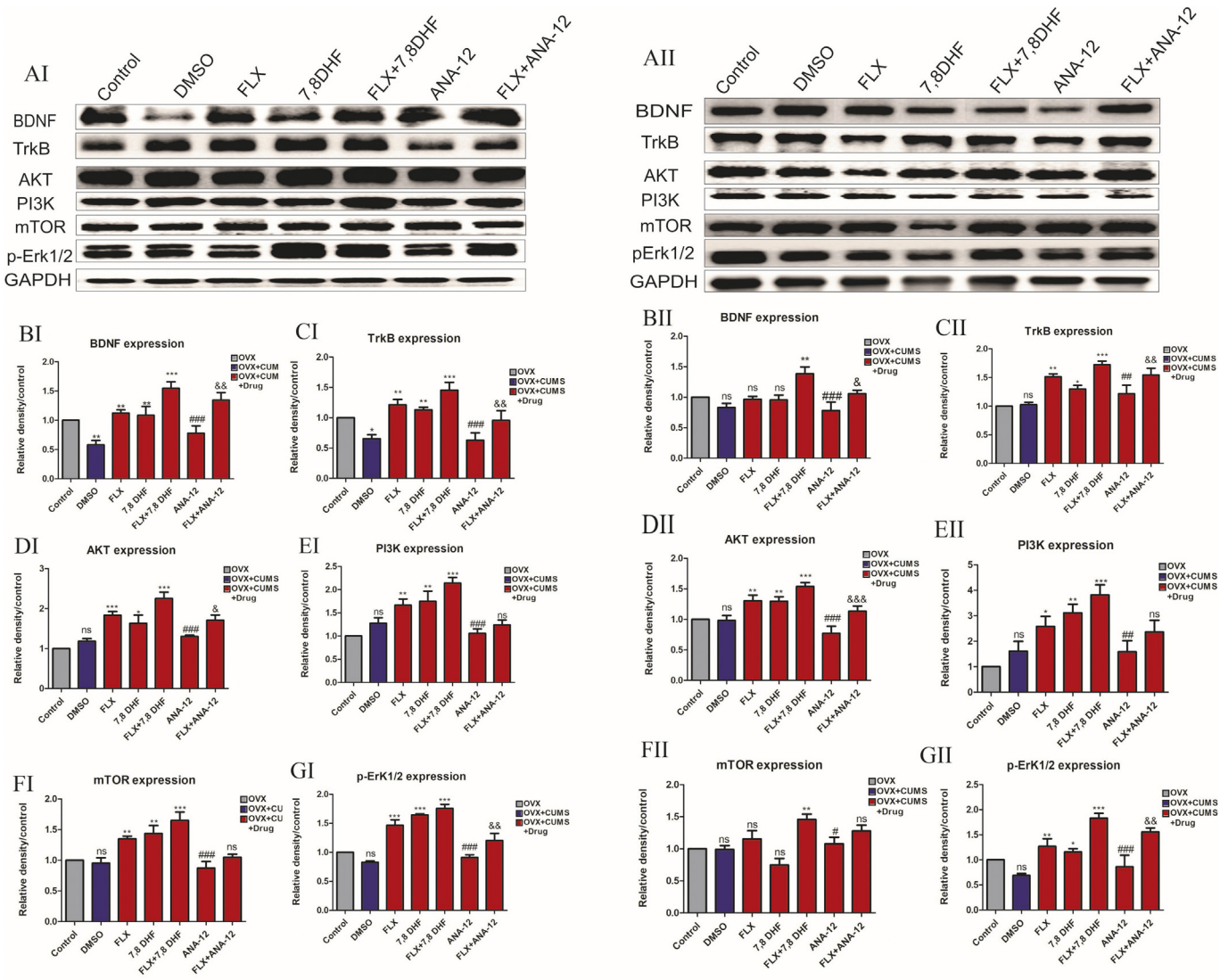

Fig. 2. I,II Effect of FLX + 7, 8 DHF treatment on BDNF/TrkB, PI3K/Akt/mTOR and phosphorylated Erk1/2 signaling pathways. Quantification analysis of (B) BDNF (C) TrkB (D) AKT (E) PI3K (F) mTOR and (G) p-ErK1/2. All values are expressed as mean ± SEM. BDNF expression in hippocampus; BDNF ($F_{6,\ 14}$ = 10.003), TrkB ($F_{6,\ 14}$ = 8.501), Akt ($F_{6,\ 14}$ = 12.935), PI3K ($F_{6,\ 14}$ = 8.432), mTOR ($F_{6,\ 14}$ = 10.075), and p-Erk1/2 ($F_{6,\ 14}$ = 29.483), FLX + 7, 8 DHF vs. DMSO& control;$^{***}P < .001$, ANA-12 vs. FLX + 7.8 DHF: $^{\#\#\#}P < .001$, BDNF expression in cortex; FLX + 7, 8 DHF vs. control& DMSO groups;$^{***}P < .001$, ANA-12 vs. FLX + 7.8 DHF: $^{\#\#\#}P < .001$.TrkB expression in hippocampus; FLX + 7, 8 DHF vs. DMSO; $P < .001$, ANA-12 vs. FLX + 7, 8 DHF: $^{\#\#\#}P < .001$. In cortex, BDNF ($F_{6,\ 14}$ = 5554), TrkB ($F_{6,\ 14}$ = 9.850), Akt ($F_{6,\ 14}$ = 10.271), PI3K ($F_{6,\ 14}$ = 6.767), mTOR ($F_{6,\ 14}$ = 6.494), and p-Erk1/2 (cortex $F_{6,\ 14}$ = 11.370), FLX + 7, 8 DHF vs. control & DMSO; $^{***}P < .001$, ANA-12 vs. FLX + 7, 8 DHF: $^{\#\#}P < .01$, FLX + ANA-12 vs. ANA-12; $P < .05$. PI3K/AKT/mTOR expression in hippocampus; FLX + 7, 8 DHF vs. DMSO& control: $^{**}P < .001$, ANA-12 vs. FLX + 7, 8 DHF: $^{\#\#\#}P < .001$, PI3K & mTOR: FLX& 7, 8 DHF vs. control and DMSO groups;$^{**}P < .01$. In cortex, PI3K/AKT/mTOR expression; FLX + 7, 8 DHF vs. DMSO & control: $^{**}P < .001$, AKT: ANA-12 vs. FLX + 7, 8 DHF: $^{\#\#\#}P < .001$, FLX& 7, 8 DHF vs. DMSO& control: $^{**}P < .01$. mTOR: FLX + 7, 8 DHF vs. control& DMSO;$^{**}P < .01$,ANA-12 vs. FLX + ANA-12;$^{\#}P < .05$. P-Erk1/2 level in hippocampus: FLX + 7, 8 DHF vs. DMSO& control: $^{***}P < .001$, ANA-12 vs. FLX + 7, 8 DHF; $^{\#\#\#}P < .01$, FLX + ANA-12 vs. ANA-12; $^{\&\&}P < .01$. In cortex, FLX + 7, 8 DHF vs. control and DMSO groups $^{**}P < .01$, ANA-12 vs. FLX + 7, 8 DHF; $^{\#\#\#}P < .001$.

notable decrease of sucrose consumption compared with FLX + 7, 8 DHF group ($P < .01$).

3.2. Effect of FLX + 7, 8 DHF treatment on BDNF/TrkB, PI3K/Akt/mTOR and phosphorylated Erk1/2 signaling pathways

Fig. 2 IA shows that both BDNF and TrkB expressions in the hippocampus of the DMSO mice were declined when compared with control group ($P < .01$ and $P < .05$). But, the FLX + 7, 8 DHF group demonstrated a marked increase in the BDNF and TrkB expressions compared with DMSO group in cortex ($F_{6,\ 14}$ = 5.554, $P < .01$ and $F_{6,\ 14}$ = 10.003, $P < .001$) and hippocampus ($F_{6,\ 14}$ = 9.850, $P < .001$and $F_{6,\ 14}$ = 8.501, $P < .001$), respectively (Fig. 2IB&C and IIB&C). The ANA-12 group presented a significant decrease in BDNF/TrkB expressions in both cortex and hippocampus ($P < .01$ and $P < .001$, respectively) compared with FLX + 7, 8 DHF group. In addition, the analyses of Akt, PI3K, mTOR, and p-Erk1/2 expressions showed a negligible change between control and DMSO groups ($P < .05$) in hippocampus and cortex (Fig. 2 ID–G & IID–G). Whereas, the established FLX + 7, 8 DHF treatment attenuated the decrease in Akt, PI3K, mTOR, and p-Erk1/2 expressions in hippocampus (Akt: $F_{6,\ 14}$ = 12.935, $P < .001$, PI3K: $F_{6,\ 14}$ = 8.432, $P < .001$, mTOR: $F_{6,\ 14}$ = 10.075, $P < .001$, p-Erk1/2: $F_{6,\ 14}$ = 29.483, $P < .001$) and cortex (Akt: $F_{6,\ 14}$ = 10.271, $P < .001$, PI3K: cortex $F_{6,\ 14}$ = 6.767,

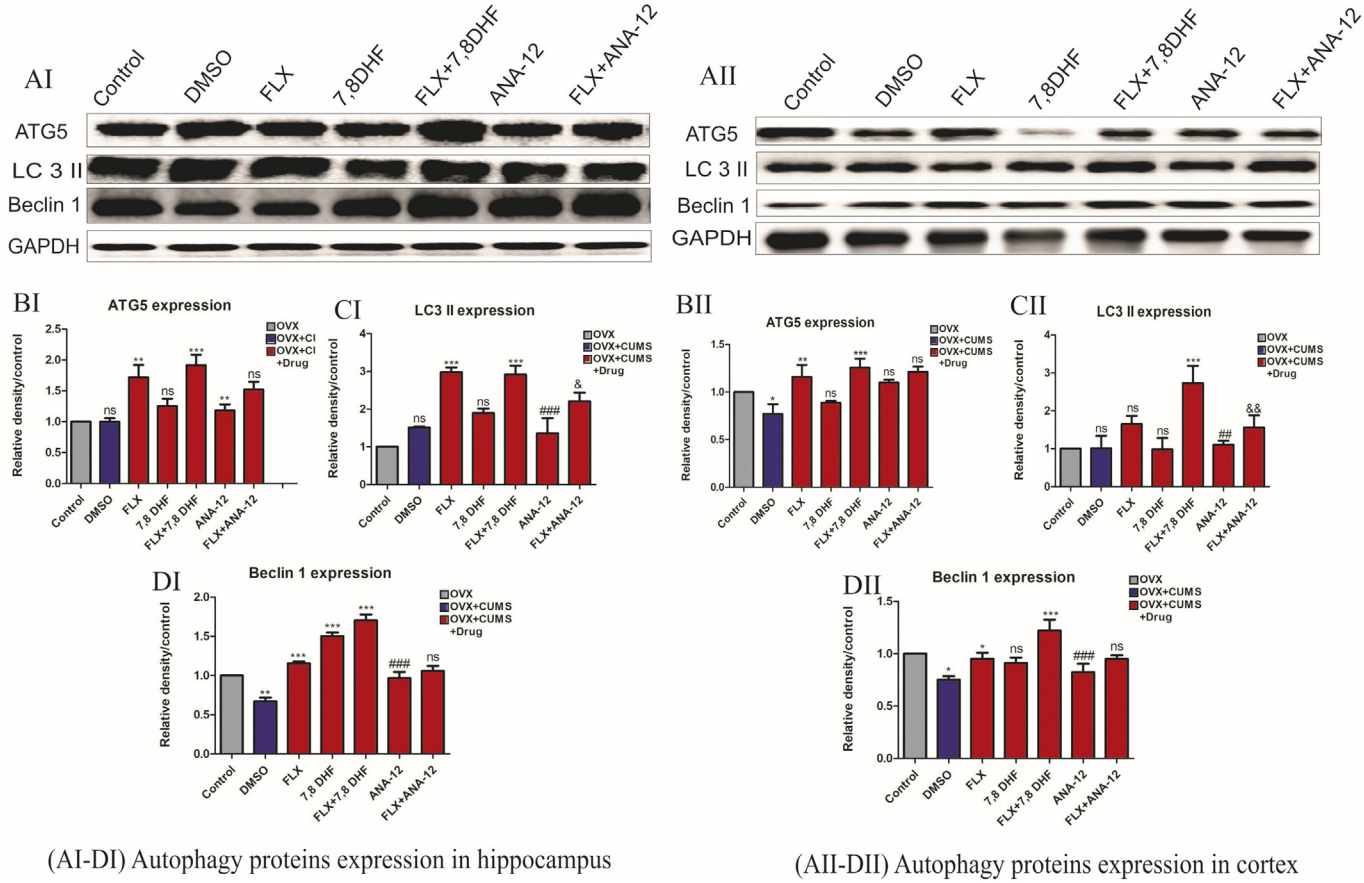

Fig. 3. I, II FLX + 7, 8 DHF treatment upregulates autophagy in selected brain region during perimenopausal period. (A) Western blot results of Atg5, LC3II, Beclin1, and GADPH. Quantification analysis of (B) Atg5, (C) LC3II, and (D) Beclin1. Values are expressed as mean ± SEM. ATG5 expression in both regions; (hippocampus; Atg5: $F_{6,\ 14} = 7.591$; LC3II: $F_{6,\ 14} = 13.291$, Beclin-1: $F_{6,\ 14} = 39.803$) (cortex; Atg5: $F_{6,\ 14} = 5.698$; LC3II: $F_{6,\ 21} = 4.997$, Beclin-1: $F_{6,\ 14} = 6.038$) FLX + 7, 8 DHF vs. DMSO & control: $^{***}P < .001$, in hippocampus ANA-12 vs. FLX + 7, 8 DHF; $^{\#\#}P < .01$, in cortex; P = ns. LC3 expression in hippocampus; FLX + 7, 8 DHF vs. control and DMSO: $^{***}P < .001$, ANA-12 vs. FLX + 7, 8 DHF; $^{\#\#\#}P < .001$, in cortex ANA-12 vs. FLX + 7, 8 DHF; $^{\#\#}P < .01$, FLX + 7, 8 DHF vs. control & DMSO; $^{***}P < .001$, ANA-12 vs. FLX + 7, 8 DHF; $^{\#\#}P < .01$. Beclin expression in hippocampus; FLX + 7, 8 DHF vs. control& DMSO groups: $^{***}P < .001$, ANA-12 vs. FLX + 7, 8 DHF; $^{\#\#\#}P < .001$, in cortex, FLX + 7, 8 DHF vs. DMSO & control: $^{***}P < .001$, ANA-12 vs. FLX + 7, 8 DHF; $^{\#\#\#}P < .001$.

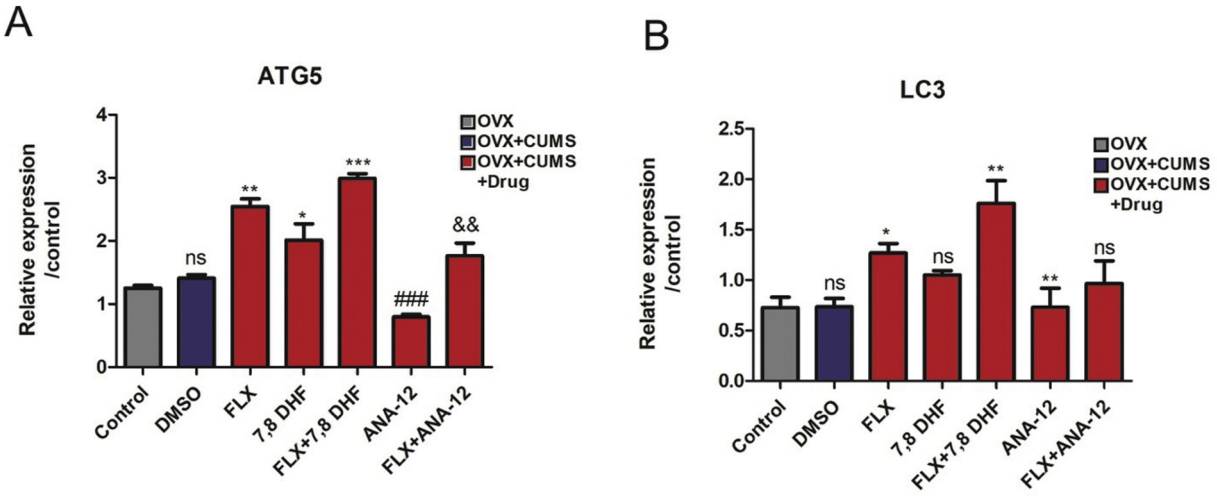

Fig. 4. Quantitative gene analysis for autophagy proteins. (A) ATG5. (B) LC3. All values are control: Atg5 ($F_{6,\ 7} = 29.743$) and LC3 ($F_{6,\ 7} = 6.161$), $^{*}P < .05$, FLX + 7, 8 DHF vs. DMSO& control:$^{***}P < .001$, ANA-12 vs. FLX + 7, 8 DHF:$^{\#\#\#}P < .001$, FLX + ANA-12 vs. ANA-12;$^{\&\&}P < .01$.(B) LC3II; FLX vs. DMSO& control:$^{*}P < .05$, FLX + 7, 8 DHF vs. DMSO, control, FLX& 7, 8 DHF:$^{**}P < .01$, ANA-12 vs. FLX + 7, 8 DHF:**P < .01.expressed as mean ± SEM. (A) ATG5; FLX vs. DMSO& control:$^{**}P < .01$, 7, 8 DHF vs. DMSO& control.

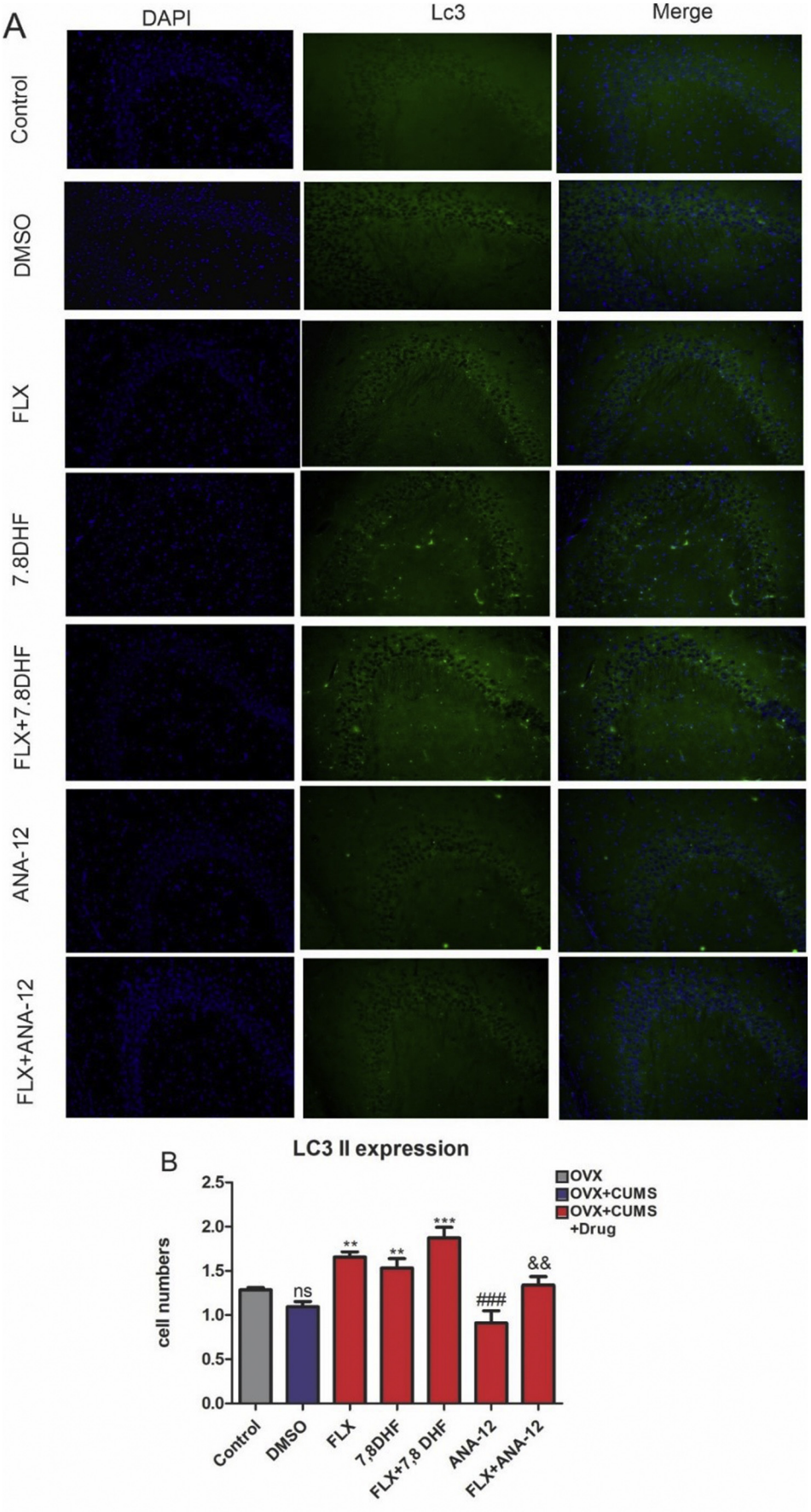

(caption on next page)

Fig. 5. LC3 II expression in hippocampus by immunofluorescence staining. (A) Immunofluorescence staining of LC3II antibody. (B) LC3 expression. All values are expressed as mean ± SEM. $F_{6, 14} = 12.052$, DMSO vs. control: ns, FLX + 7, 8 DHF vs. DMSO: $^{**}P < .01$, FLX + 7, 8 DHF vs. DMSO: $^{***}P < .001$, ANA-12 vs. FLX + 7.8 DHF: $^{\#\#\#}P < .001$, FLX + ANA-12 vs. ANA-12: $P < .01$.

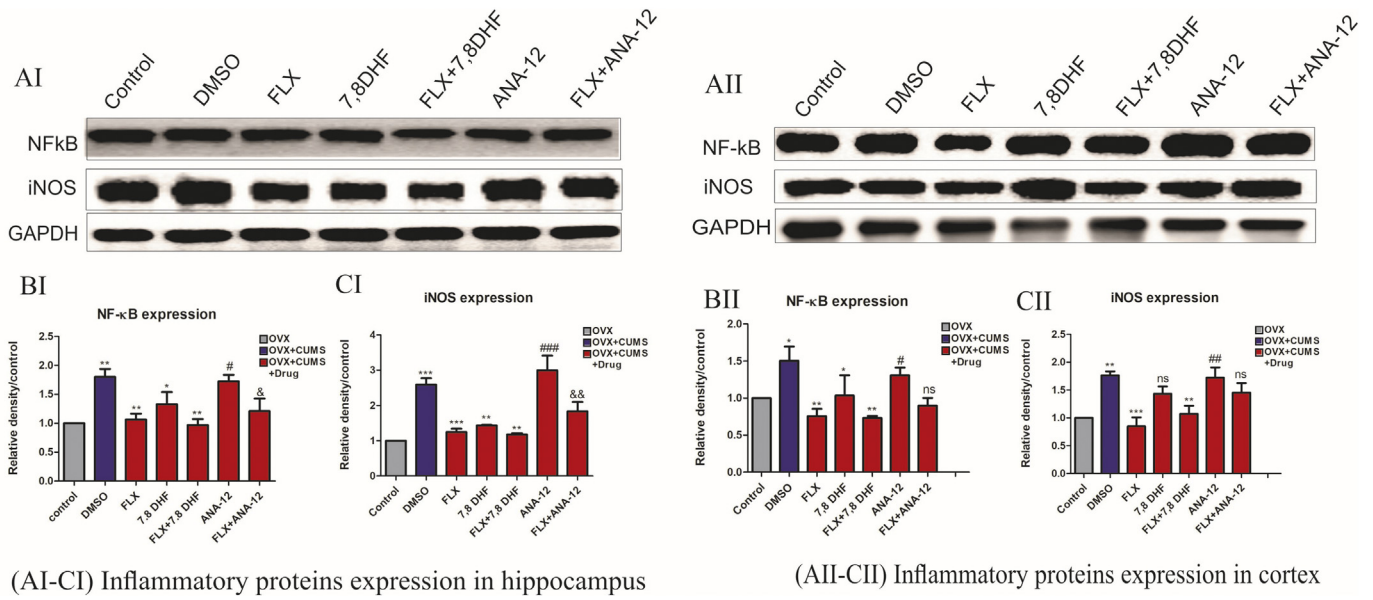

Fig. 6. I, II FLX + 7, 8 DHF treatment alleviates inflammation in mice during the perimenopausal period. (A) Western blot results of NF-kB, iNOS and GAPDH. (B)NF-kB, (C) iNOS. All values are expressed as mean ± SEM. NF-kB ($F_{6, 14} = 5.603$) and iNOS ($F_{6, 14} = 14.377$) expression in hippocampus; NF-kB; FLX + 7, 8 DHF vs. DMSO: $^{**}P < .01$, ANA-12 vs. FLX + 7, 8 DHF: $^{\#}P < .05$, iNOS; FLX + 7, 8 DHF vs. DMSO: $^{**}P < .01$, ANA-12 vs. FLX + 7.8 DHF: $^{\#\#\#}P < .001$. In cortex, NF-kB: ($F_{6, 14} = 3.900$), FLX + 7, 8 DHF vs. DMSO: $^{**}P < .01$, ANA-12 vs. FLX + 7, 8 DHF: $^{\#}P < .05$. iNOS; ($F_{6, 14} = 6.714$), FLX + 7, 8 DHF vs. DMSO: $^{**}P < .01$, ANA-12 vs. FLX + 7, 8 DHF; $^{\#\#}P < .01$.

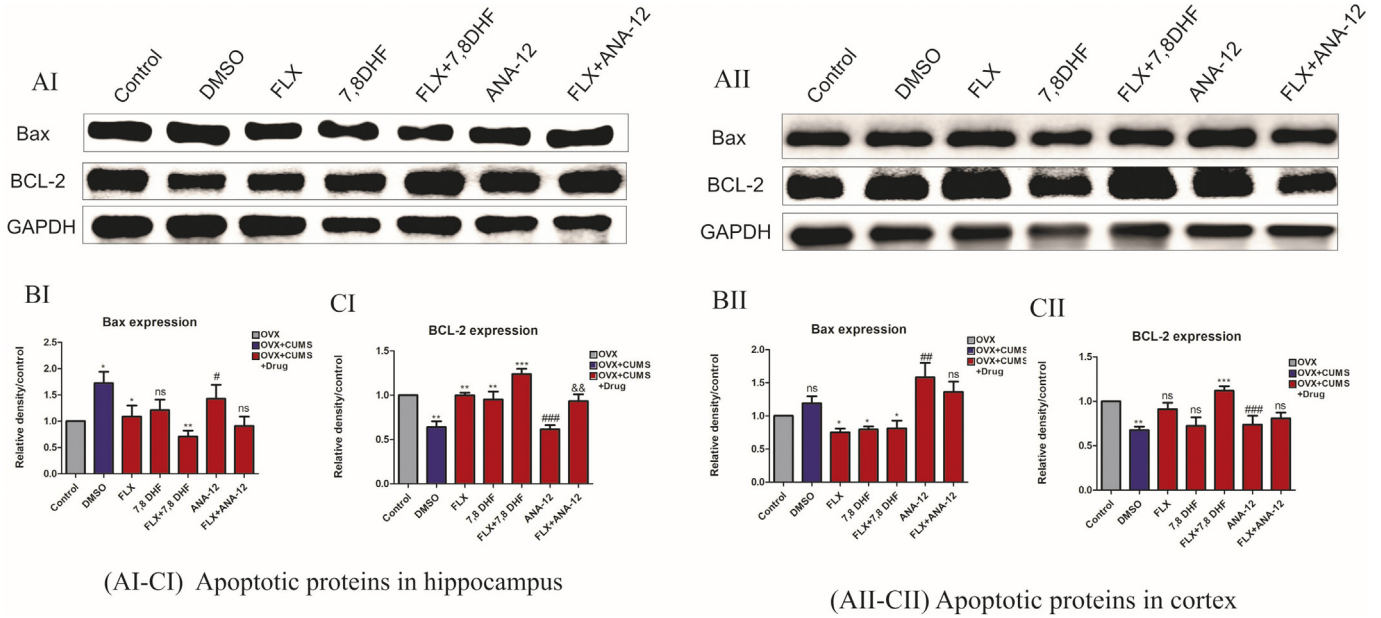

Fig. 7. I, II Effect of FLX + 7, 8 DHF treatment on apoptosis in the selected brain regions during the perimenopausal period. (A) Western blot results of Bax, Bcl-2 and GAPDH. (B) Bax, (C) Bcl-2. All values are expressed as mean ± SEM. Bax expression in hippocampus; $F_{6, 14} = 3.288$, FLX + 7, 8 DHF vs. DMSO: $^{**}P < .01$, ANA-12 vs. FLX + 7, 8 DHF: $^{\#}P < .05$. In cortex; $F_{6, 14} = 6.898$, FLX, 7, 8 DHF &FLX + 7, 8 DHF vs. DMSO: $^{*}P < .05$, ANA-12 vs. FLX + 7, 8 DHF: $^{\#\#}P < .01$. BCl-2 in hippocampus and cortex; ($F_{6, 14} = 13.721$, $F_{6, 14} = 7.033$) FLX + 7, 8 DHF vs. DMSO; $^{***}P < .001$, in hippocampus & cortex, ANA-12 vs. FLX + 7, 8 DHF:$^{\#\#\#}P < .001$ in both regions.

$P < .001$, mTOR: cortex $F_{6, 14} = 6.494$, $P < .01$, p-Erk1/2: cortex $F_{6, 14} = 11.370$, $P < .001$) compared to those of DMSO group ($P < .001$) (Fig. 2 ID–G & IID–G).

3.3. FLX + 7, 8 DHF treatment upregulates autophagy in selected brain region during perimenopausal period

To confirm the synergistic role of FLX + 7, 8 DHF treatment on autophagy mechanism, the Atg5, LC3II, and Beclin-1 levels in both

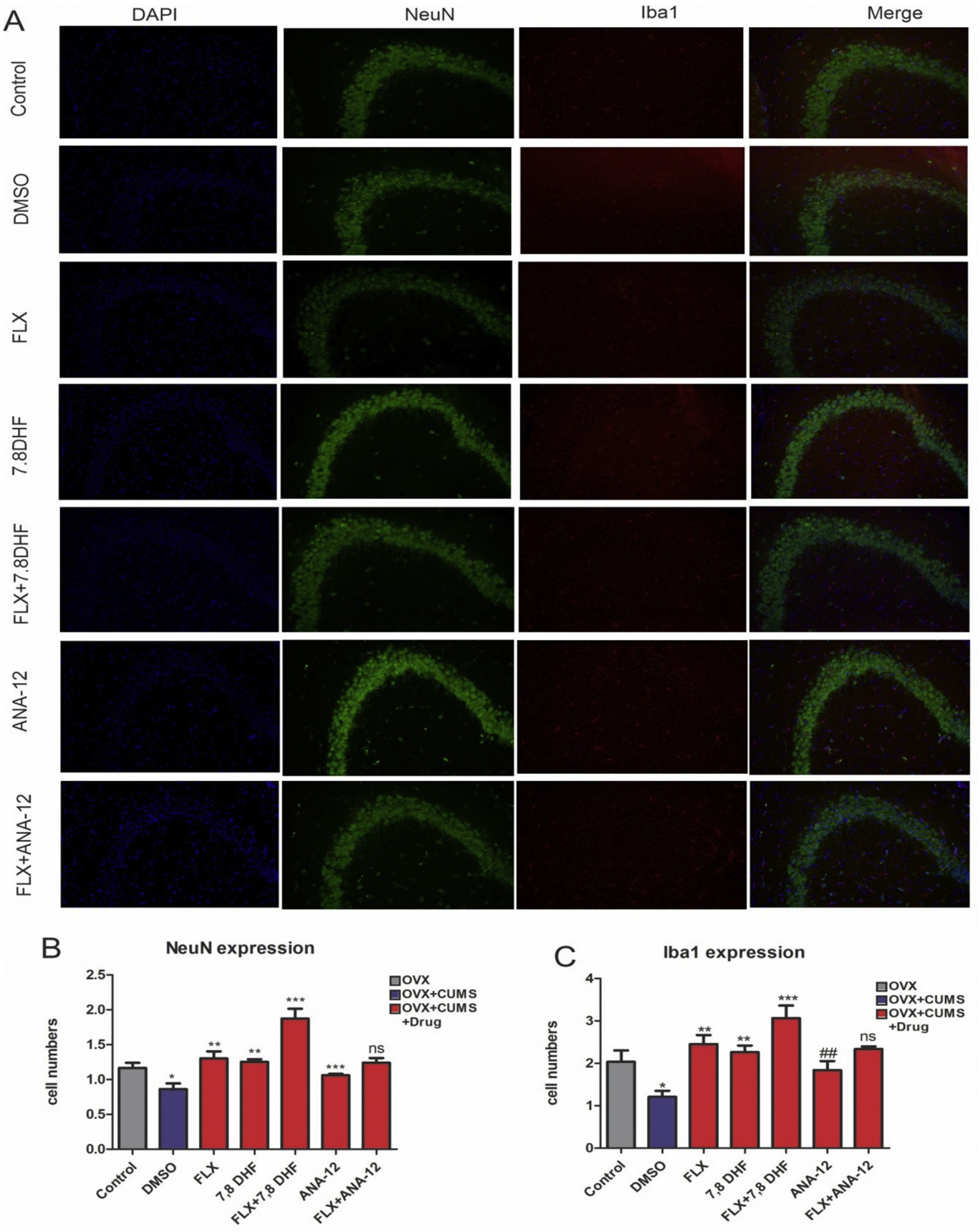

Fig. 8. Effect of FLX+7, 8 DHF treatment on alterations of Neurons and microglia in the mice hippocampus during the perimenopausal period. (A) Immunofluorescence staining of both NeuN and Iba-1 antibody. (B) NeuN expression. (C) Iba-1 expression. All values are expressed as mean ± SEM. NeuN: $F_{6, 14} = 13.904$, DMSO vs. control:$^{*}P < .05$, FLX &7, 8 DHF vs. DMSO: $^{**}P < .01$, FLX+7, 8 DHF vs. DMSO: $^{***}P < .001$, ANA-12 vs. FLX+7.8 DHF: $^{\#\#\#}P < .001$. (C) Iba-1 expression. Iba-1: $F_{6, 14} = 7.639$, DMSO vs. control:$^{*}P < .05$, FLX&7, 8 DHF vs. DMSO;$^{**}P < .01$, FLX+7, 8 DHF vs. DMSO: $^{***}P < .001$, ANA-12 vs. FLX +7, 8 DHF: $^{\#\#}P < .01$.

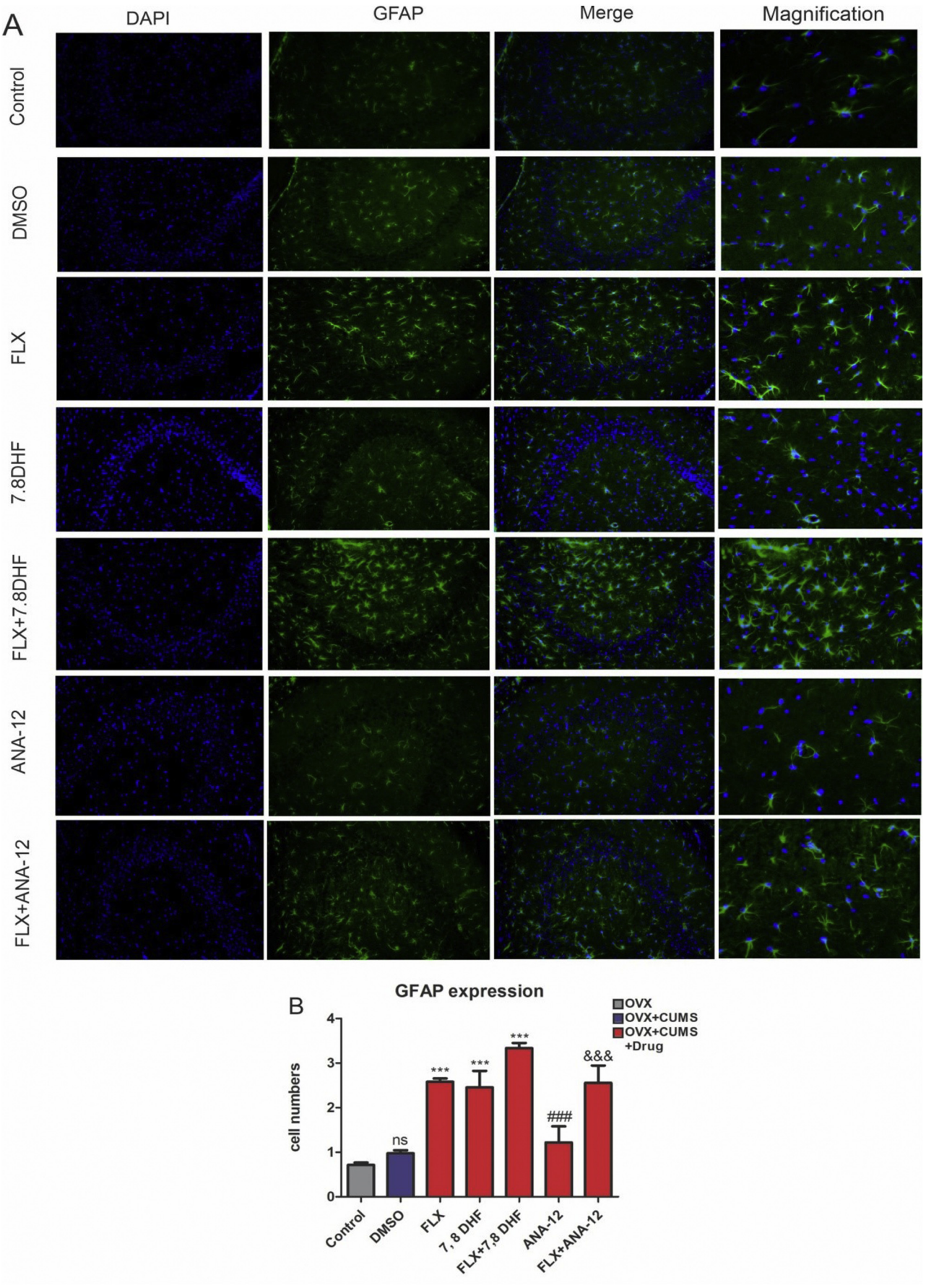

(caption on next page)

Fig. 9. Effect of FLX+7,8DHF treatment on Glial fibrillary acidic protein (GFAP) in the mice hippocampus during the perimenopausal period. (A) Immunofluorescence staining of GFAP antibody. (B)GFAP expression. All values are expressed as mean ± SEM. $F_{6, 14} = 15.528$, FLX+7, 8 DHF vs. DMSO: $^{***}P < .001$, ANA-12 vs. FLX+7.8 DHF: $^{###}P < .001$.

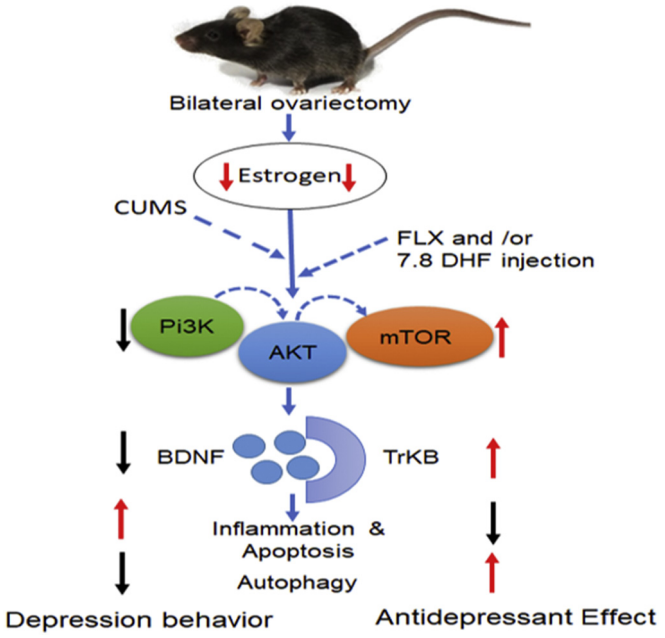

Scheme 2. Illustrative mechanism for the effect of FLX+7, 8 DHF administration to alleviate the depressive like-behavior during perimenopausal period.

hippocampus and cortex of mice were further evaluated as shown in Fig. 3 I&II. Results indicated a significant enhancement of Atg5, LC3II and Beclin-1 expressions in hippocampus of FLX+7, 8 DHF group compared with those of DMSO group (Atg5: $F_{6, 14} = 7.591$, $P < .001$; LC3II: $F_{6, 14} = 13.291$, P < .001, Beclin-1: $F_{6, 14} = 39.803$, $P < .001$) (Fig. 3IB–D). Similarly, a significant upregulation of these proteins' expressions was clearly observed in cortex FLX+7, 8 DHF group when compared with that of DMSO group (Atg5: $F_{6, 14} = 5.698$, $P < .001$; LC3II: $F_{6, 21} = 4.997$, $P < .001$, Beclin-1: $F_{6, 14} = 6.038$, $P < .001$) (Fig. 3IIB–D). On the other hand, the autophagy proteins expressions of ANA-12 mice displayed decreased level compared with FLX+7, 8 DHF group (Fig. 3IIB–D). To distinguish whether the enhancement in autophagy proteins levels is due to the increase in their gene expressions, qPCR technique was used to analyze the expression of Atg5 and LC3 genes in hippocampus. Although the Atg5 and LC3 gene expressions manifested non obvious contrast in case of control and DMSO groups, the FLX+7, 8 DHF group showed elevated upregulation of Atg5 ($F_{6, 7} = 29.743$, $P < .001$) and LC3 ($F_{6, 7} = 6.161$, $P < .01$) genes compared with DMSO group (Fig. 4). Under the condition of autophagosomal accumulation, the immunofluorescence signals will increase and show puncta due to increased LC3 expressions and such phenomenon can be clearly noticed in FLX+7, 8 DHF group when compared with that of DMSO group ($F_{6, 14} = 12.052$, $P < .001$) (Fig. 5). These findings correlate well with the western blot results.

3.4. FLX+7, 8 DHF treatment alleviates inflammation in mice during the perimenopausal period

Alleviating inflammation represents a critical feature to access the effectiveness of therapy. Both NF-kB and iNOS expressions in hippocampus displayed higher levels in DMSO group than those in control group ($F_{6, 14} = 5.603$, $P < .01$ for NF-kB and $P < .001$ for iNOS) (Fig. 6IB–C). In comparison to DMSO group, FLX+7, 8 DHF mice showed conspicuous decrease of NF-kB and iNOS expressions in hippocampus ($F_{6, 14} = 5.603$, P < .01, $F_{6, 14} = 14.377$, $P < .01$) and cortex ($F_{6, 14} = 3.900$, $P < .01$, $F_{6, 14} = 6.714$, $P < .01$), respectively (Fig. 6IB–C & IIB–C). On the other hand, a notable increase of iNOS level was observed in hippocampus of ANA-12 group ($F_{6, 14} = 14.377$, $P < .001$) and cortex ($F_{6, 14} = 6.714$, $P < .01$) (Fig. 6IC & IIC). Also, the NF-kB of ANA-12 mice was considerably increased in hippocampus ($P < .05$) and cortex ($P < .05$) compared to that of FLX+7, 8 DHF mice (Fig. 6IB & IIB).

3.5. Effect of FLX+7, 8 DHF treatment on apoptosis in the selected brain region during the perimenopausal period

Bax and Bcl-2 proteins in both hippocampus and cortex were employed to evaluate apoptosis. The FLX+7, 8 DHF group revealed an interesting increase in Bcl-2 expression in both hippocampus and cortex ($F_{6, 14} = 13.721$, $P < .001$, $F_{6, 14} = 7\ 0.033$, $P < .001$) and a remarkable decrease in Bax ($F_{6, 14} = 3.288$, $P < .01$ in hippocampus and $F_{6, 14} = 6.898$, $P < .05$ in cortex) compared with those of DMSO group. While, a high level of Bax expression ($P < .05$) and a low level of Bcl-2 expression ($P < .001$) were obtained for ANA-12 group compared with those of FLX+7, 8 DHF group in both hippocampus and cortex (Fig. 7 IA–C & II-A–C).

3.6. Effect of FLX+7, 8 DHF treatment on alterations of neurons and microglia in the mice hippocampus during the perimenopausal period

The brain immunofluorescence slices staining of NeuN (green) and Iba1 (red) were adopted to address the changes in neuron and microglia as depicted in Fig. 8. Our collected results indicated that FLX+7, 8 DHF group possessed high signals of NeuN and Iba1 expressions compared to those of control ($P < .001$) and DMSO groups ($P < .001$). But weak signals of NeuN and Iba1 expressions were existed in ANA-12 group compared to those of FLX+7, 8 DHF group (NeuN: $F_{6, 14} = 13.904$, Iba-1: $F_{6, 14} = 7.639$) (Fig. 8B&C).

3.7. Effect of FLX+7, 8 DHF treatment on Glial fibrillary acidic protein (GFAP) in the mice hippocampus the perimenopausal period

Astrocyte activation after FLX+7, 8 DHF treatment was probed by GFAP antibody as presented in Fig. 9. The expression of GFAP protein ($F_{6, 14} = 15.528$) was greatly improved in 7,8 DHF + FLX group compared to that of control ($P < .001$) and DMSO groups ($P < .001$), while a significant decrease of GFAP expression was recorded for ANA-12 mice compared to that of 7,8 DHF + FLX group ($P < .001$) (Fig. 9).

4. Discussion

Over the past three decades, FLX has been emerged as an effective antioxidant, anti-inflammatory, and as well as neuro-protection drug (Caiaffo et al., 2016). However, its capability to treat depressed patients still needs more attention. In this work, we demonstrate the effectiveness of FLX as an antidepressant drug when combined with 7, 8 DHF as a TrkB agonist treatment to induce antidepressant-like activity during perimenopausal period in the CUMS paradigm. Such role was mediated via the PI3K/Akt/mTOR signaling pathway. Results evidenced the activity of the proposed FLX+7, 8 DHF treatment and its role to intrinsically regulate the associated parameters such as apoptosis, autophagy, and anti-inflammatory proteins (Scheme 2).

The CUMS-induced depressive-like behavior of mice was corroborated by the behavioral assessments, namely SPT and FST according to the previously reported literature [Tan et al., 2018; Yang et al., 2017]. Anhedonia and distressed behaviors are depressive indicators that can

Table 2
Summary of outcomes analyzed for the optimized groups.

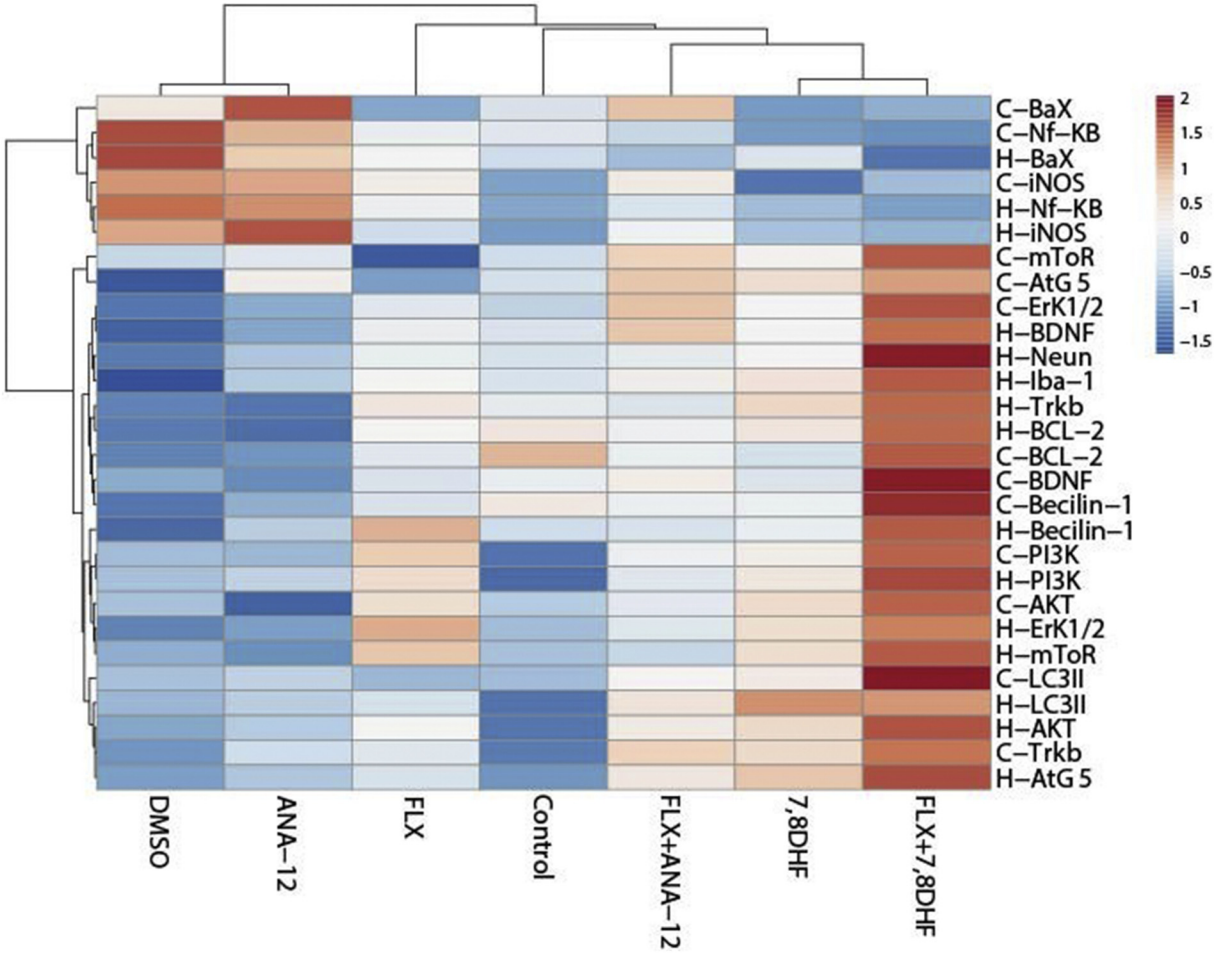

be experimentally assessed by SPT and FST, respectively [Yang et al., 2018]. Results showed that the administration of FLX + 7, 8 DHF treatment could sufficiently alleviate anhedonia-like behavior and minimize the immobility rate that induced by CUMS.

In the brain, BDNF/TrkB play a vital role in a synaptic transmission neural regeneration, synaptic plasticity, and neurogenesis. In the present study, we found that the expression levels of BDNF/TrkB in hippocampus and cortex of DMSO group were significantly down-regulated. Previous studies reported the fundamental relationship between both BDNF-TrkB signaling, antidepressants action, and major depression disorder (MDD) pathway [Cazorla et al., 2011; Agacayak et al., 2015]. It is well known that the BDNF protein can alleviate the depression symptoms throughout its interaction with TrkB. Such BDNF-TrkB integration leads to activate some signaling pathways including extracellular signal-regulated kinase 1/2 (ERK1/2) [Lin et al., 2014; He et al., 2015]. Our findings demonstrated that perimenopausal-induced depressive symptoms and the consequent down-regulation of BDNF/TrkB/ERK1/2 and AKT/PI3K/mTOR signaling could be reversed by FLX + 7, 8 DHF administration. This implies that the BDNF expression can be improved by FLX + 7, 8 DHF combinational treatment through ameliorating TrkB/ ERK1/2 pathway and AKT/PI3K/mTOR, leading to an antidepressant-like effect. Such observation corroborates with the previous reports that indicated a degraded level of p-ERK1/2 in stressed animals [Meller et al., 2003; Qi et al., 2008] and an elevated level after antidepressant administration [Cui et al., 2016].

The P-ERK1/2 protein has a great impact in modulation of neuronal function and possesses a substantial role in regulating learning and memory [Colucci-D'amato et al., 2003; Kandel, 2001]. The reported data indicated a reduction of both BDNF/TrkB/ERK1/2 and AKT/PI3K/mTOR proteins in hippocampus and cortex after ANA-12 administration. This observation agrees well with that presented by Zhang.et al. The results elucidated that the ANA-12 could act as a therapeutic agent for patients suffering from high BDNF-TrkB levels due to its unique capability to modify this signaling into a decreased level [Zhang et al., 2014; Zhang et al., 2015]. It is well known that a high autophagy activity can slow down or prohibit the pathological symptoms of neurodegenerative disease because of its capability to control energy homeostasis [Amin et al., 2019;Decressac et al., 2013]. Moreover, the induction and regulation of the autophagy process can be achieved via the mechanism of rapamycin (mTOR) and phosphatidylinositol 3-kinase (PI3K) complex proteins[Hurley and Young, 2017; Ktistakis and Tooze, 2016]. Accordingly, our observations showed that the CUMS model applied upon ovariectomized mice could down regulate the main autophagy markers (ATG5/LC3II). This reduction was revoked following FLX + 7, 8 DHF administration, implying that the combined treatment can sufficiently improve autophagy proteins by influencing the mTOR/PI3K expression. Also, the administration of ANA-12 could minimize the autophagy proteins (ATG5/LC3II), which matches well with that presented by Menzies and coworkers. The authors claimed that the reduction of essential autophagy genes in mice models led to neuronal dystrophy owing to the formation of toxic intra and extra cellular proteins aggregation [Menzies et al., 2017]. Besides, the pathological features of neurodegenerative diseases could be suppressed or even prevented throughout increasing autophagy activity after FLX administration [Yang et al., 2017; Tan et al., 2018].

FLX has been established as a robust anti-inflammatory drug when

either administrated as a sole drug or combined with another drug [Koo et al., 2010]. Despite the crucial impact of inflammation in disease progress, its specific role in depression is yet to be clarified. Koo et al., suggested that the activation of NF-kB signaling can take part into stress and chronic stress-induced depressive-like behavior was via NF-kB signaling[Koo et al., 2010]. These proteins were control DNA transcription and involved in cellular responses to stimuli such as stress, cytokines, and as well as processes of synaptic plasticity and memory [Meffert et al., 2003]. In the current study, analysis revealed that both NF-kB and iNOS expressions upregulated significantly in both hippocampus and cortex following CUMS implemented on ovariectomized mice. However, these expressions were significantly down-regulated following administration of FLX + 7, 8 DHF treatment. On the other hand, ANA-12 administration elevated the expression of inflammatory proteins in both brain regions.

Reported data demonstrated that chronic stress could increase the susceptibility of certain populations of neurons to cell death, while antidepressant treatment showed a superior ability to antagonize these effects and promote neuro-protection (Mckernan et al., 2009). Our results confirmed that ANA-12 treatment following CUMS implemented on ovariectomized mice could up-regulate Bax expression and down-regulate Bcl-2 expression, but these levels were reversed after FLX + 7, 8 DHF administration.

Previous studies suggested that FLX administration could enhance the neurogenesis process in hippocampus and thus alleviate the depression-like behavior in stressed animal models and patients [Lee et al., 2001; Santarelli et al., 2003]. Changes in microglia reflect the immune response against invading pathogens by antigen release [Colton, 2009]. Moreover, the stress can significantly restrain microglia in hippocampus, however this effect inhibition might possibly be modified with antidepressant drugs [Tong et al., 2017]. Recent works displayed a down-regulation in NeuN expression after CUMS and up-regulation of this expression in hippocampus after FLX administration [Wang et al., 2008; Tan et al., 2018]. Our results elucidated that the combined FLX + 7, 8 DHF treatment could attenuate the inhibition of NeuN and Iba-1 expressions in hippocampus after applying CUMS on ovariectomized mice. The previously introduced results illustrated that the BDNF expression in hippocampal astrocytes could regulate the GFAP expression and the decrease of GFAP level was strongly correlated with the major depression disorder (MDD) [Quesseveur et al., 2013]. The present work showed a low level of GFAP expression in depressed group, while a high level was noticed following FLX + 7, 8 DHF administration. Such observation is consistent with that obtained by Duric and coworkers. The analyses displayed a decrease of the GFAP expression in hippocampal region of MDD patients [Duric et al., 2010; Duric et al., 2013].

To summarize, the investigation of combined FLX + 7, 8 DHF treatment to ameliorate depressive-like symptoms during the perimenopausal period was well addressed (Table 2). The study confirmed that the adjunction of 7, 8 DHF to FLX can provide a fast antidepressant-like effect in perimenopausal model. The effectiveness of the proposed therapy could by realized via PI3/Akt/mTOR/ERK signaling pathway. Therefore, it is likely that the optimized therapy may produce an efficient antidepressant effect in patients with MDD.

Authors' contributions

ZH and MF designed the study. NA drafted the manuscript. NA, SX, XT and YC performed the experiments, analyzed the data. ZH, SH, YM, QR and BB revised the manuscript. All authors read and approved the final manuscript.

Funding

The National Natural Science Foundation of China (grant numbers 81871063 and 81971769) and the Zhejiang Public Welfare Technology Application Research Program (experimental animals) (grant number 2016C37096) supported this study.

Declaration of Competing Interest

The authors declare no known conflicts of interest.

Acknowledgment

We appreciate the technical assistance provided by the Core Facilities of Zhejiang University Institute of Neuroscience.

References

Agacayak, E., Basaranoglu, S., Tunc, S.Y., Icen, M.S., Findik, F.M., Kaplan, I., Evliyaoglu, O., Gul, T., 2015. Oxidant/antioxidant status, paraoxonase activity, and lipid profile in plasma of ovariectomized rats under the influence of estrogen, estrogen combined with progesterone, and genistein. Drug Des. Devel. Ther. 9, 2975–2982.

Amin, Z., Gueorguieva, R., Cappiello, A., Czarkowski, K.A., Stiklus, S., Anderson, G.M., Naftolin, F., Epperson, C.N., 2006. Estradiol and tryptophan depletion interact to modulate cognition in menopausal women. Neuropsychopharmacology. 31, 2489–2497.

Amin, N., Tan, X., Ren, Q., Zhu, N., Botchway, B.O.A., Hu, Z., Fang, M., 2019. Recent advances of induced pluripotent stem cells application in neurodegenerative diseases. Prog. Neuro-Psychopharmacol. Biol. Psychiatry 95, 109674.

Borrow, A.P., Cameron, N.M., 2014. Estrogenic mediation of serotonergic and neurotrophic systems: implications for female mood disorders. Prog. Neuro-Psychopharmacol. Biol. Psychiatry 54, 13–25.

Caiaffo, V., Oliveira, B.D.R., De sá, F.B., Evêncio Neto, J., 2016. Anti-inflammatory, antiapoptotic, and antioxidant activity of fluoxetine. Pharmacol. Res. Perspect. 4, e00231.

Can, A., Dao, D.T., Arad, M., Terrillion, C.E., Piantadosi, S.C., Gould, T.D., 2012. The mouse forced swim test. J. Vis. Exp. 59, e3638.

Cazorla, M., Prémont, J., Mann, A., Girard, N., Kellendonk, C., Rognan, D., 2011. Identification of a low-molecular weight TrkB antagonist with anxiolytic and antidepressant activity in mice. J. Clin. Invest. 121, 1846–1857.

Choo, M., Miyazaki, T., Yamazaki, M., Kawamura, M., Nakazawa, T., Zhang, J., Tanimura, A., Uesaka, N., Watanabe, M., Sakimura, K., Kano, M., 2017. Retrograde BDNF to TrkB signaling promotes synapse elimination in the developing cerebellum. Nat. Commun. 8, 195.

Colton, C.A., 2009. Heterogeneity of microglial activation in the innate immune response in the brain. J. NeuroImmune Pharmacol. 4, 399–418.

Colucci-D'amato, L., Perrone-Capano, C., Di Porzio, U., 2003. Chronic activation of ERK and neurodegenerative diseases. Bioessays. 25, 1085–1095.

Cui, Jingqiu, Yang, Kun, Yu, Xue, Wang, Jing-lan, Li, Jie, Zhang, Yong, Li, Hengfen, 2016. Chronic Fluoxetine treatment upregulates the activity of the ERK1/2-NF-κB signaling pathway in the hippocampus and prefrontal cortex of rats exposed to forced-swimming stress. Med Princ Pract. 25 (6), 539–547.

Davis, S.R., Lambrinoudaki, I., Lumsden, M., Mishra, G.D., Pal, L., Rees, M., Santoro, N., Simoncini, T., 2015. Menopause. Nat. Rev. Dis. Primers. 1, 15004.

Decressac, M., mattsson, B., Weikop, P., Lundblad, M., Jakobsson, J., Björklund, A., 2013. TFEB-mediated autophagy rescues midbrain dopamine neurons from α-synuclein toxicity. Proc. Natl. Acad. Sci. U. S. A. 110, E1817–E1826.

Dunlop, B.W., Davis, P.G., 2008. Combination treatment with benzodiazepines and SSRIs for comorbid anxiety and depression: a review. Prim. Care Companion J. Clin. Psychiatry. 10, 222–228.

Duric, V., Banasr, M., Licznerski, P., Schmidt, H.D., Stockmeier, C.A., Simen, A.A., Newton, S.S., Duman, R.S., 2010. A negative regulator of MAP kinase causes depressive behavior. Nat. Med. 16, 1328–1332.

Duric, V., Banasr, M., Stockmeier, C.A., Simen, A.A., Newton, S.S., Overholser, J.C., Jurjus, G.J., Dieter, L., Duman, R.S., 2013. Altered expression of synapse and glutamate related genes in post-mortem hippocampus of depressed subjects. Int. J. Neuropsychopharmacol. 16, 69–82.

Fiske, A., Wetherell, J.L., Gatz, M., 2009. Depression in older adults. Annu. Rev. Clin. Psychol. 5, 363–389.

Greenberg, P.E., Stiglin, L.E., Finkelstein, S.N., Berndt, E.R., 1993. The economic burden of depression in 1990. J. Clin. Psychiatry 54, 405–418.

Greendale, G.A., Derby, C.A., Maki, P.M., 2011. Perimenopause and cognition. Obstet. Gynecol. Clin. N. Am. 38, 519–535.

Harte-Hargrove, L.C., Maclusky, N.J., Scharfman, H.E., 2013. Brain-derived neurotrophic factor-estrogen interactions in the hippocampal mossy fiber pathway: implications for normal brain function and disease. Neuroscience. 239, 46–66.

He, Q., Wang, S., Liu, X., Guo, H., Yang, H., Zhang, L., Zhuang, P., Zhang, Y., Ye, Z., Hu, L., 2015. Salvianolate lyophilized injection promotes post-stroke functional recovery via the activation of VEGF and BDNF-TrkB-CREB signaling pathway. Int. J. Clin. Exp. Pathol. 8, 108–122.

Hiemke, C., Hartter, S., 2000. Pharmacokinetics of selective serotonin reuptake inhibitors. Pharmacol. Ther. 85, 11–28.

Hurley, J.H., Young, L.N., 2017. Mechanisms of autophagy initiation. Annu. Rev. Biochem. 86, 225–244.

Janssen, I., Powell, L.H., Crawford, S., Lasley, B., Sutton-Tyrrell, K., 2008. Menopause and

the metabolic syndrome: the study of women's health across the nation. Arch. Intern. Med. 168, 1568–1575.
Jezierski, M.K., Sohrabji, F., 2001. Neurotrophin expression in the reproductively senescent forebrain is refractory to estrogen stimulation. Neurobiol. Aging 22, 309–319.
Kandel, E.R., 2001. The molecular biology of memory storage: a dialogue between genes and synapses. Science. 294, 1030–1038.
Koo, J.W., Russo, S.J., Ferguson, D., Nestler, E.J., Duman, R.S., 2010. Nuclear factor-kappaB is a critical mediator of stress-impaired neurogenesis and depressive behavior. Proc. Natl. Acad. Sci. U. S. A. 107, 2669–2674.
Krishna, G., Agrawal, R., Zhuang, Y., Ying, Z., Paydar, A., Harris, N.G., Royes, L.F.F., Gomez-Pinilla, F., 2017. 7,8-Dihydroxyflavone facilitates the action exercise to restore plasticity and functionality: implications for early brain trauma recovery. Biochim. Biophys. Acta-Mol. Basis Dis. 1863, 1204–1213.
Krishnan, V., Nestler, E.J., 2008. The molecular neurobiology of depression. Nature. 455, 894–902.
Ktistakis, N.T., Tooze, S.A., 2016. Digesting the expanding mechanisms of autophagy. Trends Cell Biol. 26, 624–635.
Lee, H.J., Kim, J.W., Yim, S.V., Kim, M.J., Kim, S.A., Kim, Y.J., Kim, C.J., Chung, J.H., 2001. Fluoxetine enhances cell proliferation and prevents apoptosis in dentate gyrus of maternally separated rats. Mol. Psychiatry 6, 725–728.
Lin, P., Wang, C., Xu, B., Gao, S., Guo, J., Zhao, X., Huang, H., Zhang, J., Chen, X., WANG, Q., Zhou, W., 2014. The VGF-derived peptide TLQP62 produces antidepressant-like effects in mice via the BDNF/TrkB/CREB signaling pathway. Pharmacol. Biochem. Behav. 120, 140–148.
Liu, M.Y., Yin, C.Y., Zhu, L.J., Zhu, X.H., Xu, C., Luo, C.X., Chen, H., Zhu, D.Y., Zhou, Q.G., 2018. Sucrose preference test for measurement of stress-induced anhedonia in mice. Nat. Protoc. 13, 1686–1698.
Marken, P.A., Munro, J.S., 2000. Selecting a selective serotonin reuptake inhibitor: clinically important distinguishing features. Primary Care Companion J. Clin. Psychiatry. 2, 205–210.
Mckernan, D., Dinan, T., Cryan, J., 2009. “killing the blues”: a role for cellular suicide (apoptosis) in depression and the antidepressant response? Prog. Neurobiol. 88, 246–263.
Meffert, M.K., Chang, J.M., Wiltgen, B.J., Fanselow, M.S., Baltimore, D., 2003. NF-kappa B functions in synaptic signaling and behavior. Nat. Neurosci. 6, 1072–1078.
Meller, E., Shen, C., Nikolao, T.A., JENSEN, C., Tsimberg, Y., Chen, J., Gruen, R.J., 2003. Region-specific effects of acute and repeated restraint stress on the phosphorylation of mitogen-activated protein kinases. Brain Res. 979, 57–64.
Menzies, F.M., Fleming, A., Caricasole, A., Bento, C.F., Andrews, S.P., Ashkenazi, A., Füllgrabe, J., Jackson, A., Jimenez Sanchez, M., Karabiyik, C., Licitra, F., Lopez Ramirez, A., Pavel, M., Puri, C., Renna, M., Ricketts, T., Schlotawa, L., Vicinanza, M., Won, H., Zhu, Y., Skidmore, J., Rubinsztein, D.C., 2017. Autophagy and neurodegeneration: pathogenic mechanisms and therapeutic opportunities. Neuron 93, 1015–1034.
Perez-lopez, F.R., Perez-Roncero, G., Fernandez-Inarrea, J., Fernandez-Alonso, A.M., Chedraui, P., Llaneza, P., 2014. Resilience, depressed mood, and menopausal symptoms in postmenopausal women. Menopause 21, 159–164.
Prior, J.C., 2005. Ovarian aging and the perimenopausal transition. Endocrine. 26, 297–300.
Qi, X., Lin, W., Li, J., Li, H., Wang, W., Wang, D., Sun, M., 2008. Fluoxetine increases the activity of the ERK-CREB signal system and alleviates the depressive-like behavior in rats exposed to chronic forced swim stress. Neurobiol. Dis. 31, 278–285.
Quesseveur, G., David, D.J., Gaillard, M.C., Pla, P., Wu, M.V., Nguyen, H.T., Nicolas, V., Auregan, G., David, I., Dranovsky, A., Hantraye, P., Hen, R., Gardier, A.M., Déglon, N., Guiard, B.P., 2013. BDNF overexpression in mouse hippocampal astrocytes promotes local neurogenesis and elicits anxiolytic-like activities. Transl. Psychiatry 3, e253.
Santarelli, L., Saxe, M., Gross, C., Surget, A., Battaglia, F., Dulawa, S., Weisstaub, N., Lee, J., Duman, R., Arancio, O., Belzung, C., Hen, R., 2003. Requirement of hippocampal neurogenesis for the behavioral effects of antidepressants. Science. 301, 805–809.
Singh, M., Meyer, E.M., Simpkins, J.W., 1995. The effect of ovariectomy and estradiol replacement on brain-derived neurotrophic factor messenger ribonucleic acid expression in cortical and hippocampal brain regions of female Sprague-dawley rats. Endocrinology. 136, 2320–2324.
Sohrabji, F., Miranda, R.C., Toran-Allerand, C.D., 1995. Identification of a putative estrogen response element in the gene encoding brain-derived neurotrophic factor. Proc. Natl. Acad. Sci. U. S. A. 92, 11110–11114.
Tan, X., Du, X., Jiang, Y., Botchway, B.O.A., Hu, Z., Fang, M., 2018. Inhibition of autophagy in microglia alters depressive-like behavior via bdnf pathway in postpartum depression. Front. Psychiatry 9, 434.
Tatiana, A.G., Polina, P., Alexey, V.T., Sergey, B.S., 2019. The low molecular weight brain-derived neurotrophic factor mimetics with antidepressant-like activity. Curr. Pharm. Des. 25, 729–737.
Tong, L., Gong, Y., Wang, P., Hu, W., Wang, J., Chen, Z., Zhang, W., Huang, C., 2017. Microglia loss contributes to the development of major depression induced by different types of chronic stresses. Neurochem. Res. 42, 2698–2711.
Wang, J.W., David, D.J., Monckton, J.E., Battaglia, F., Hen, R., 2008. Chronic fluoxetine stimulates maturation and synaptic plasticity of adult-born hippocampal granule cells. J. Neurosci. 28, 1374–1384 2008.
Willner, P., Towell, A., Sampson, D., Sophokleous, S., Muscat, R., 1987. Reduction of sucrose preference by chronic unpredictable mild stress, and its restoration by a tricyclic antidepressant. Psychopharmacology. 93, 358–364.
Yang, Y., Hu, Z., Du, X., Davies, H., Huo, X., Fang, M., 2017. miR-16 and fluoxetine both reverse autophagic and apoptotic change in chronic unpredictable mild stress model rats. Front. Neurosci. 11, 428.
Yang, Y., Cui, Y., Sang, K., Dong, Y., Ni, Z., Ma, S., Hu, H., 2018. Ketamine blocks bursting in the lateral habenula to rapidly relieve depression. Nature 554, 317–322.
Zhang, J.C., Wu, J., Fujita, Y., Yao, W., Ren, Q., Yang, C., Li, S.X., Shirayama, Y.H., Ashimoto, K., 2014. Antidepressant effects of TrkB ligands on depression-like behavior and dendritic changes in mice after inflammation. Int. J. Neuropsychopharmacol. 18 pyu077.
Zhang, J.C., Yao, W., Dong, C., Yang, C., Ren, Q., Ma, M., Han, M., Hashimoto, K., 2015. Comparison of ketamine, 7,8-dihydroxyflavone, and ANA-12 antidepressant effects in the social defeat stress model of depression. Psychopharmacology 232, 4325–4335.
Zhang, M.W., Zhang, S.F., Li, Z.H., Han, F., 2016. 7,8-Dihydroxyflavone reverses the depressive symptoms in mouse chronic mild stress. Neurosci. Lett. 635, 33–38.
Zhou, J., Zhang, H., Cohen, R.S., Pandey, S.C., 2005. Effects of estrogen treatment on expression of brain-derived neurotrophic factor and cAMP response element-binding protein expression and phosphorylation in rat amygdaloid and hippocampal structures. Neuroendocrinology 81, 294–310.
Zhu, H., Nan, S., Suo, C., Zhang, Q., Hu, M., Chen, R., Wan, J., Li, M., Chen, J., Ding, M., 2019. Electro-acupuncture affects the activity of the hypothalamic-pituitary-ovary axis in female rats. Front. Physiol. 10, 466.